Published in final edited form as:
Arch Toxicol. 2021 May ; 95(5): 1631–1645. doi:10.1007/s00204-021-03014-2.

Development and Validation of the TGx-HDACi Transcriptomic Biomarker to Detect Histone Deacetylase Inhibitors in Human TK6 Cells

Eunnara Cho[1,2], **Andrea Rowan-Carroll**[1], **Andrew Williams**[1], **J. Christopher Corton**[3], **Heng Hong Li**[4,5], **Albert Fornace Jr.**[4,5], **Cheryl Hobbs**[6], **Carole L. Yauk**[1,7,*]

[1]Environmental Health Science and Research Bureau, Health Canada, Ottawa, ON, Canada

[2]Department of Biology, Carleton University, Ottawa, ON, Canada

[3]Center for Computational Toxicology and Exposure, US-EPA, Research Triangle Park, NC, United States

[4]Department of Oncology, Lombardi Comprehensive Cancer Center, Georgetown University Medical Center, Washington, D.C., United States

[5]Department of Biochemistry and Molecular and Cellular Biology, Georgetown University Medical Center, Washington, D.C., United States

[6]Integrated Laboratory Systems LLC, Research Triangle Park, NC, United States

[7]Department of Biology, University of Ottawa, Ottawa, ON, Canada

Abstract

Transcriptomic biomarkers can be used to inform molecular initiating and key events involved in a toxicant's mode of action. To address the limited approaches available for identifying epigenotoxicants, we developed and assessed a transcriptomic biomarker of histone deacetylase inhibition (HDACi). First, we assembled a set of 10 prototypical HDACi and 10 non-HDACi reference compounds. Concentration-response experiments were performed for each chemical to collect TK6 human lymphoblastoid cell samples after 4 hours of exposure and to assess cell viability following a 20h-recovery period in fresh media. One concentration was selected for each chemical for whole transcriptome profiling and transcriptomic signature derivation, based on cell viability at the 24-hour time point and on maximal induction of HDACi-response genes (*RGL1*, *NEU1*, *GPR183*) or cellular stress-response genes (*ATF3*, *CDKN1A*, *GADD45A*) analyzed by TaqMan qPCR assays after 4 hours of exposure. Whole transcriptomes were profiled after 4 hour exposures by Templated Oligo-Sequencing (TempO-Seq). By applying the nearest shrunken centroid (NSC) method to the whole transcriptome profiles of the reference compounds, we derived an 81-gene toxicogenomic (TGx) signature, referred to as TGx-HDACi, that classified

*To whom correspondence should be addressed: carole.yauk@uottawa.ca.

STATEMENT OF AUTHOR CONTRIBUTIONS

CLY and EC designed the study with important intellectual and technical input from AW, HHL, AFJ, and CH. CLY obtained funding to support the project. EC and ARC conducted the cellular exposures and cell viability measurements. EC extracted RNA samples and performed qPCR and TempO-Seq. AW conducted the statistical analyses and prepared figures. JCC conducted the Running Fisher test and prepared the methods and results sections for this analysis. EC prepared the manuscript with intellectual input from all authors. All authors had access to the study data and approved the final manuscript.

all 20 reference compounds correctly using NSC classification and the Running Fisher test. An additional four HDACi and seven non-HDACi were profiled and analyzed using TGx-HDACi to further assess classification performance; the biomarker accurately classified all 11 compounds, including three non-HDACi epigenotoxicants, suggesting a promising specificity toward HDACi. The availability of TGx-HDACi increases the diversity of tools that can facilitate mode of action analysis of toxicants using gene expression profiling.

INTRODUCTION

Early gene expression changes in response to a toxicant provide insight into the molecular initiating events (MIE) and key events (KE) involved in its mode of action (MOA). Transcriptomic signatures, or biomarkers, typically consist of a panel of genes that robustly and consistently respond to stressors belonging to specific mechanistic classes. Such biomarkers provide a pragmatic method for efficiently extracting mechanistic information from high-content transcriptomic data and can be used to detect early molecular perturbations that are predictive of chemical hazards. Therefore, increasing the diversity of available transcriptomic biomarkers will facilitate rapid screening of chemicals to identify potential MOAs and prioritize follow-up tests in toxicological assessment.

A study by Li et al. (2015a, b) generated DNA microarray gene expression profiles of TK6 human lymphoblastoid cells exposed to 28 agents for 4 hours (Li et al. 2015a, b). TGx-DDI, a 64-gene toxicogenomic (TGx) biomarker of DNA damage-inducing (DDI) agents, was derived from these gene expression profiles of 13 DDI and 15 non-DDI reference agents. Four histone deacetylase inhibitors (HDACi), oxamflatin, trichostatin A, apicidin, and HC toxin (Helminthosporium carbonum toxin), were among the non-DDI agents in this initial training set. A very distinct expression pattern was observed for the four HDACi by visual inspect of a heatmap produced on 1628 genes that were perturbed by more 1.7-fold for at least one of the 28 agents used in TGx-DDI development. This expression pattern appeared to clearly distinguish the HDACi agents from the remaining compounds with various MOA such as topoisomerase inhibitors, tubulin inhibitors, electron transport chain inhibitors, and endoplasmic reticulum disruptors (Li et al. 2015a, b; Li et al. 2017).

Previous transcriptomic studies have identified signatures of HDACi for use in different contexts within toxicity assessment. Notably, Dreser et al. (2015) and Rempel et al. (2015) developed HDACi signatures in human stem cells for detecting disruptions in neurodevelopment (i.e., inhibited migration of neural crest cells) and distinguishing HDACi from mercurial compounds, respectively. Although these signatures demonstrated predictive abilities within their respective neurodevelopmental toxicity studies, they are limited in scope for broader applications due to the required exposure length (48-h and 6-day exposures) and the use of a specialized cell line. More recently, Yeakley et al. (2017) identified genes that were consistently responsive to trichostatin A, a non-selective HDACi, in a Templated Oligo-Sequencing (TempO-Seq) gene expression analysis of five cell types (MCF-7, PC-3, undifferentiated HL-60, and two differentiation states of HL-60) that were exposed for 6 h (Yeakley et al. 2017). The Li et al. (2015a, b) and Yeakley et al. (2017)

studies indicated that it may be possible to develop a transcriptomic biomarker of HDACi that can be measured after short exposures *in vitro* for applications in chemical screening.

Post-translational modification (PTM) of histones is one of the ways in which gene expression is regulated epigenetically; the N-terminus tails of histones are transiently methylated, phosphorylated, and/or acetylated, which alters nucleosome stability and the binding configuration of histones and DNA (Biswas et al. 2011; Audia and Campbell 2016). The lysine residues of histone tails are reversibly acetylated and deacetylated by histone acetyltransferases (HATs) and histone deacetylases (HDACs), respectively. The acetylation of histone tails weakens the association between histones and DNA, allowing access to DNA for transcription. Therefore, inhibiting HDACs leads to hyperacetylation of histones, prolonging the dissociation of histones and DNA, and generally leading to dysregulation of transcription (Gallinari et al. 2007; Seto and Yoshida 2013).

The 18 known human HDACs are organized into four classes based on the sequence homology shared with yeast deacetylases. Classes I, II, and IV HDACs are Zn^{2+}-dependent and class III HDACs are NAD^{+}-dependent in their catalytic activities (Seto and Yoshida 2013). Class II is further divided into classes IIa and IIb. Protein expression and activity levels differ across the four main classes and the two sub-classes within class II based on tissue and cellular localization (Morris and Monteggia 2014; Wright and Menick 2016; Millard et al. 2017; Rajan et al. 2018). Class I HDACs are ubiquitously expressed and are located in the nucleus, while classes II and IV contain both nuclear and cytoplasmic HDACs with tissue-specific expression patterns (Park and Kim 2020).

Along with other agents that modulate the PTM of histones, HDACi are considered epigenotoxicants. Several chemicals present in the environment, such as methoxyacetic acid, resveratrol, and butyrate, have been identified as HDACi (Wade et al. 2008; Ventrelli et al. 2013; Chang et al. 2014). The downstream effects of HDACi exposure are broad due to the diverse roles that HDACs play in the cell; the effects of HDACi include activation of pro-apoptotic genes, disruption in cell cycle, and inhibition of DNA repair (Bose et al. 2014). Dysregulation of PTM of histones has implications in developmental toxicity, neurotoxicity, and carcinogenesis (Audia and Campbell 2016).

In the present study, we identified and tested a transcriptomic biomarker of HDACi, named TGx-HDACi, to address the limited tools available for identifying toxicants that operate through the inhibition of HDAC as the MIE. To do this, we expanded on the original TGx-DDI sample sets in TK6 cells, with a long-term vision to enable rapid screening for genotoxicity and epigenotoxicity using a single high-throughput transcriptomic analysis. We first constructed a reference compound set containing HDACi and non-HDACi chemicals. The HDACi chemical set was limited to the inhibitors of the classical, Zn^{2+}-dependent human HDACs that constitute HDAC classes I (HDACs 1 to 3 and 8), II (HDACs 4 to 7, 9, and 10) and IV (HDAC 11); these HDACi contain Zn-binding groups and inhibit HDACs by chelating the Zn from the active site (Zhang et al. 2018). Sirtuins, the NAD^{+}-dependent class III HDACs, are not affected by these HDACi and, thus, require a different class of chemicals for inhibition (Seto and Yoshida 2013). To provide an adequate representation of both the HDACi and non-HDACi classes while keeping the training set at a reasonable size and

balanced between the two chemical classes, we focused on the inhibition of classical, Zn^{2+}-dependent HDACs for HDACi biomarker derivation. Gene expression profiling was applied to cells exposed to HDACi and non-HDACi chemicals using TempO-Seq (BioSpyder). The TempO-Seq platform was selected because it is amenable to working on cell lysates in 96- and 384-well format, enabling high-throughput application for chemical screening. The nearest shrunken centroid (NSC) method was applied to the whole transcriptome profiles of the reference compounds to derive the TGx-HDACi biomarker (Tibshirani et al. 2002). The performance of TGx-HDACi was evaluated by classifying an external validation compound set containing HDACi, non-HDACi, and non-HDACi epigenetic modulators (inhibitors of histone acetylase, histone methyltransferase, and histone demethylase), using different statistical analyses (probability analysis using NSCs, principal component analysis, hierarchical clustering, and running Fisher test).

MATERIALS AND METHODS

Chemicals

The list of compounds in the reference set (10 HDACi and 10 non-HDACi) and in the external validation set (four HDACi and seven non-HDACi), the tested and selected concentrations, and the manufacturers are summarized in Tables 1 and 2. The HDACi compounds were selected based on published reviews on HDACi and commercial availability (Bose et al. 2014; Damaskos et al. 2017). The non-HDACi were chosen to span multiple MOA from the set of 28 agents used to develop the TGx-DDI biomarker by Li et al. (2015a, b). An additional three chemicals that are non-HDACi epigenetic modulators (histone demethylase, methyltransferase, and acetyltransferase) were included in the external validation set (Balasubramanyam et al. 2004; Girard et al. 2014; Lochmann et al. 2018).

Cell Culture and Treatments

Existing RNA samples from TK6 cells treated with three HDACi (oxamflatin, HC toxin, and apicidin), and 10 non-HDACi reference compounds, that were produced in a previous study (Cho et al. 2019) were used alongside new samples generated for the present work; the older RNA samples were produced in 2015 and stored at −70°C until this study in 2018. The oxamflatin and apicidin samples were included in the HDACi reference set for biomarker derivation and the HC toxin samples were included in the external validation set. The samples of the remaining eight HDACi reference compounds and ten external validation compounds (three HDACi and seven non-HDACi) were newly generated. The Cho et al. (2019) study was an extension of the TGx-DDI biomarker work by Li et al. (2015a, b). Chemical concentration selection and cell exposure methods for these samples are described by Li et al. (2015a, b). The concentration selection for the remaining chemicals was based on a modification of that approach (described further below). Cell culture and exposure methods described herein are consistent with the 2019 study.

TK6 cells (ATCC# CRL-8015; ATCC, Manassas, VA) were cultured in suspension in RPMI1640 medium (Gibco) supplemented with 10% v/v heat-inactivated horse serum (Gibco; New Zealand origin) and 200 μg/mL sodium pyruvate (Gibco), at 37°C and 5% CO_2. The density was maintained between $1x10^5$ and $1x10^6$ cells/mL in a T75 flask.

In the range finding experiments for concentration selection, TK6 cells in 96-well or 6-well plates were exposed to eight to ten concentrations of each compound in two technical replicates for 4 hours to measure cell viability at the 24-hour time point (post 20-hour recovery in media) or to extract RNA for qPCR analyses. The tested concentration ranges of reference and validation compounds are listed in Tables 1 and 2, respectively. The cells were exposed to each compound prepared in their respective vehicle solvents (1% water, dimethyl sulfoxide (DMSO), or methanol (MeOH) v/v in medium) at a density of 4 $x10^5$ - $5x10^5$ cells/mL.

In the definitive study, TK6 cells were exposed to each compound at the selected concentrations for 4 hours on three separate occasions to generate three replicates of RNA samples for whole transcriptome profiling.

Cell Viability Measurement by MTT Assay

Cell viability was measured using the 3-(4,5-dimethylthiazol-2-yl)-2,5-diphenyltetrazolium bromide (MTT) assay (R&D Systems, Minneapolis, MN) after 4-hour exposures followed by 20 hours of recovery in medium at 37°C, on a SpectraMax microplate reader (Molecular Devices). Cell viability was calculated as the percentage of viable cells in treatments compared to vehicle control.

Total RNA Extraction and Quantitative Reverse Transcription PCR

TK6 cells were harvested after 4-hour exposures to all compounds. Total RNA was extracted and purified using the RNeasy Mini Kit (Qiagen, Toronto, ON, Canada) following the manufacturer's protocol. The quantity and quality of each extracted RNA sample was assessed using a NanoDrop ND-100 spectrophotometer (Thermo Scientific, Burlington, ON, Canada) and an Agilent 2100 Bioanalyzer or an Agilent TapeStation (Agilent Technologies, Mississauga, ON, Canada). All RNA samples had A260/280 absorbance ratios of ≥2.0 and RNA integrity number (RIN) between 7.5 and 10.

The concentration optimization method used by (Li et al. 2015a, b) was modified to select the HDACi treatment concentrations for whole transcriptome profiling. The concentration-response of three genes, *RGL1*, *NEU1*, and *GPR183* (referred to as the "HDACi indicator genes"), was measured in two technical replicates using TaqMan gene expression assays (Applied Bioscience, Burlington, Canada). These three genes were selected because: (1) they had the largest fold change in expression in TK6 cells following exposure to four HDACi (oxamflatin, trichostatin A, HC toxin, and apicidin) and (2) they were not altered by any of the non-HDACi exposures (Li et al. 2015a, b). Specifically, *RGL1* and *NEU1* were upregulated and *GPR183* was downregulated across the four HDACi. The concentration that induced the highest fold changes in the three indicator genes after 4-hour exposure, without overt cytotoxicity in the MTT assay after a 20h-recovery (less than 50% reduction in viability at 24 h) was identified and selected for each chemical for whole transcriptome profiling.

For non-HDACi compounds, the concentration-responses of the three stress response indicator genes used by (Li et al. 2015a, b) (*ATF3, GADD45A,* and *CDKN1A*) were measured in two technical replicates. *GUSB* was measured in all samples for normalization.

The delta-delta Ct method was used to normalize and calculate the fold change in the indicator genes (Vandesompele et al. 2002). Again, the concentration that induced the highest fold changes in these three indicator genes after 4-hour exposure, without overt cytotoxicity in the MTT assay after a 20h-recovery (less than 50% reduction in viability at 24 h) was identified and selected for each chemical.

HDAC Enzyme Activity Assay

A FLUOR DE LYS® HDAC fluorometric cellular activity assay kit (Enzo Life Sciences, Farmingdale, NY) was used to measure relative HDAC enzyme activity levels in TK6 cells treated (n=3) with the 20 reference compounds and 11 external validation compounds at the selected concentrations for 4 hours, to confirm that the compounds are either HDACi or non-HDACi in TK6 cells at these concentrations. Briefly, as per the manufacturer's protocol, TK6 cells were plated in a 96-well plate at a density of 1 $x10^5$ cells/well in 99 μL of RPMI medium without phenol red containing the FLUOR DE LYS HDAC substrate. In each well, 1 μL of the treatment solution was added, resulting in a final concentration of 1 % v/v in the medium. The cells were treated with each compound and vehicle solvent in triplicates. Fluorescence of the deacetylated product generated from the reaction between HDAC and the FLUOR DE LYS enzyme substrate was measured (Ex. 360 nm, Em. 460 nm) using a SpectraMax Gemini microplate reader (Molecular Devices) after 4 hours of exposure. HDAC enzyme activity levels were measured as arbitrary fluorescence units (AFU).

Whole Transcriptome Profiling

Two 96-sample TempO-Seq Human Whole Transcriptome Assay kits (BioSpyder, Carlsbad, CA) were used to generate sequencing libraries using total RNA from TK6 cells following the manufacturer's protocols (Yeakley et al. 2017). Three replicates, each generated from cells exposed on different days, were used for the whole transcriptome analysis of each chemical. One 96-well plate was loaded with the reference compound samples and the HDACi validation samples. Existing samples of TSA were sequenced with this batch, but these data were omitted because the transcriptional responses in the three replicates of TSA were low and did not contribute to biomarker derivation. It is possible that the treatment concentration of 66 nM was insufficient to induce robust transcriptional responses. Thus, concentration selection for TSA was repeated using the approach described above and 300 nM was selected for generating three new replicates. The second 96-well plate was loaded with the non-HDACi validation samples and the newly generated TSA samples. The libraries were prepared approximately 5 months apart. On each 96-well plate, 2 replicates of negative control (water only), human universal reference RNA, and human brain total RNA were included for quality control and assessment. Each RNA sample (approximately 100 ng/μL) was diluted in an equal volume of the 2 × TempO-Seq Lysis buffer to a final RNA concentration of approximately 50 ng/μL. Two μL of this mixture were used (RNA input of 100 ng) in the annealing of detection oligos (DO) to RNA, followed by the removal of unbound DOs by a nuclease and the ligation of bound DOs. The ligated DOs were amplified by PCR using tagged primers to generate sequencing libraries. Finally, the libraries were pooled and quantified by qPCR using a KAPA SYBR FAST Universal qPCR kit for Illumina sequencing platforms (Roche, Wilmington, MA). Library building failed for one of the three replicates of methotrexate (MTX) and, thus, we moved forward with two replicates for

this treatment. The pooled libraries were sequenced on an Illumina NextSeq 500 using a 75-cycle flow cell.

TempO-Seq Data Processing

The BCL files were converted to FASTQ files and the reads were demultiplexed using bcl2fastq v. 2.20.0.42. The FASTQ files were then processed using the “pete. star. Script_v3.0” (freely provided by BioSpyder with the library kits). The script uses star v.2.5 and the qCount function from QuasR to align the reads and to extract the feature counts specified in a Gene Transfer Format (GTF) file from the aligned reads, respectively. We first confirmed low signal (< 0.3%) from negative controls (water only) included on all TempO-Seq plates. We referred to boxplots of total mapped reads for each sample and hierarchical clustering of all samples to identify poor quality data and remove outliers. A dissimilarity of >0.2 with the main data set was applied as a filter to identify outliers. From this analysis, one water control, one replicate of pracinostat and one replicate of tacedinaline were removed. The median number of mapped reads for the samples in the experiment was 4.5 million; the lowest sample had 1.9 million mapped reads.

The correlation between the two replicates of human universal reference RNA and human brain reference RNA within each plate was analyzed; human brain total RNA samples had within-plate correlations of 0.997 and 0.998, and human universal reference RNA samples had a within-plate correlation of 0.999 on both plates. The correlation between the human brain reference RNA samples and the universal reference RNA samples across the two plates ranged from 0.713 to 0.735 and from 0.781 to 0.794, respectively.

Using R 3.4.1, the read counts of all samples were normalized as counts per million (CPM) (Law et al. 2014). The CPM calculated for each chemical treatment was then normalized to its vehicle control. The three replicates of each treatment were averaged. A cut-off of >9 was applied to the CPM read counts. The TempO-seq count data are available on NCBI’s Gene Expression Omnibus (GEO) under the accession number GSE164478.

Signature Derivation

The nearest shrunken centroid (NSC) method was applied to the TempO-Seq gene expression profiles of the 20 reference compounds to derive the HDACi transcriptomic signature (Hastie et al. 2001; Tibshirani et al. 2002; Li et al. 2015a, b). The NSC method was performed in the R statistical environment using the pamr function (www.bioconductor.org). Here, the standard centroids of the HDACi and non-HDACi classes was estimated by computing the mean expression level of each gene and dividing by the within-class standard deviation.

The shrinkage parameter was determined with an aim of establishing a transcriptomic biomarker containing 50–100 genes. 10-fold cross validation was employed to identify shrinkage parameters that produced gene panels within this range with classification accuracy (Hastie et al. 2001). For 10-fold cross validation, the 20 reference compounds were divided evenly into 10 groups each containing a compound from the HDACi class and the non-HDACi class. At each round within the 10-fold cross validation, one of the 10 groups was treated as the test set, while the remaining 9 groups are used to build the

classifier to classify the test set as HDACi or non-HDACi in a NSC probability analysis; compounds were assigned to the HDACi class if the probability of membership was above 90%. A cross-validation error of 1/20 (95% accuracy) was allowed to generate gene panels within the target range for size.

A shrinkage value of 3.449 was selected to generate an 81-gene panel that yielded 95% accuracy in 10-fold cross validation. We named this gene panel the TGx-HDACi transcriptomic biomarker.

External Validation

To assess the performance of the 81-gene TGx-HDACi transcriptomic biomarker, an additional 11 compounds were classified using three different statistical analyses: probability analysis, principal component analysis (PCA), and hierarchical clustering. A compound was classified as HDACi if the probability of membership in the HDACi class was above 90%. The PCA was performed using the prcomp in R (www.r-project.org) and hierarchical clustering was performed using the hclust function in R using average linkage and Euclidean distance using the TGx-HDACi gene set. A compound was classified as HDACi if it clustered with the HDACi reference methods compounds.

Classification by Running Fisher Test

The use of the Running Fisher test to determine the predictive accuracy of a transcriptomic biomarker has been described (Corton et al. 2018). Briefly, the TGx-HDACi biomarker consisting of the 81 genes and average fold-change values across all of the HDACi compounds was uploaded to the BaseSpace Correlation Engine database (URL: https://www.illumina.com/products/by-type/informatics-products/basespace-correlation-engine.html; formally NextBio) (Kupershmidt et al. 2010). The gene expression profile of each HDACi or non-HDACi compound was compared to the biomarker using the Running Fisher test. For each pairwise comparison, the P-value of the Running Fisher test and direction of the correlation were exported. p values were converted to $-\text{Log}_{10}$ (p value). The − Log10 (p value) of compounds that were negatively associated with the biomarker were converted to negative numbers by adding a minus sign to indicate negative association. The reference set of 20 compounds was used to derive a $-\text{Log}_{10}$(P-value) cut-off of 15 that separated HDACi from non-HDACi. This cut-off was then applied to the external validation set.

RESULTS

Concentration Optimization

To select the optimal concentration of each reference (training set) compound for whole transcriptome analysis, the concentration-responses of three indicator genes were measured to choose a single concentration inducing robust transcriptional responses for each chemical. *RGL1, NEU1,* and *GPR183* were measured for HDACi compounds (an example is provided in Fig. 1A), and *ATF3, GADD45A,* and *CDKN1A* were measured for non-HDACi compounds (Supplementary Fig. S1 and S4). *GPR183* was downregulated, and *RGL1* was upregulated by all 11 HDACi in a concentration-dependent manner, as

expected. While *NEU1* was upregulated by the eight non-selective, pan-HDACi, three class I-selective HDACi compounds, mocetinostat, entinostat, and tacedinaline, downregulated *NEU1* (Supplementary Fig. S1). Moreover, there was a smaller in increase in the expression of *RGN1* in these three treatments compared to pan-HDACi treatments (Fig. 1B). Cell viability was measured at the same concentrations using the MTT assay after 4-hour exposures and 20 hours of recovery in fresh medium (Supplementary Fig. S2 and S3). The selected concentrations induced the largest fold changes in their respective indicator genes without reducing cell viability below 80% at 24 h, except for AraC and docetaxel which decreased cell viability by 40% and 30%, respectively. Fig. 1B summarizes the expression levels of the three HDACi indicator genes measured after 4 hour exposures to HDACi at the selected concentrations.

HDAC Enzyme Activity Assay

HDAC enzyme activity was measured in TK6 cells treated with the 20 reference compounds and the 11 external validation compounds at the selected concentrations for 4 hours (Supplementary Fig. S5 and S6). All 10 reference HDACi and four validation HDACi significantly reduced HDAC activity compared to the vehicle control (one-way ANOVA, post-hoc Dunnett's test; p-value < 0.05). Non-HDACi compounds did not induce significant reductions in HDAC activity compared to the vehicle control, except for garcinol, a histone acetyltransferase inhibitor.

Transcriptomic Signature of HDACi

To derive a transcriptomic signature of HDACi, the NSC method was applied to the TempO-Seq whole transcriptome profiles of 20 reference compounds consisting of 10 HDACi and 10 non-HDACi. After identifying the NSC shrinkage values that yielded 95% accuracy in 10-fold cross validation, an 81-gene panel was identified that we named the TGx-HDACi transcriptomic biomarker (Supplementary Table SI).

The TGx-HDACi biomarker classified all 20 reference compounds accurately using NSC classification (Fig. 2A). The 81-gene expression profiles were further analyzed by PCA and hierarchical clustering (Fig. 3). In the PCA, the reference compounds formed two loose clusters that were separated by classes (Fig. 3; left panel), with HDACi compounds having negative PC1 and non-HDACi having positive PC1 values. Concordantly, the reference compounds branched into two clusters by class in hierarchical clustering (Fig. 3; right panel). Mocetinostat and tacedinaline, two selective inhibitors of Class I HDACs were separated from the main HDACi cluster in the scatterplot of the PCA. These two compounds also formed a separate branch within the HDACi cluster in hierarchical clustering. The overall prediction accuracy of the biomarker in classifying the reference set was 100%.

Based on correlation with the TGx-HDACi biomarker in the Running Fisher test, the 20 reference compounds were ranked by $-\text{Log}_{10}$(p-value) (Fig. 4). A $-\text{Log}_{10}$(P-value) cut-off that separated HDACi from non-HDACi was set at 15, which lay approximately halfway between the two classes. This threshold was applied to the external validation set to classify the compounds as HDACi or non-HDACi in the Running Fisher test.

External Validation

To assess the performance of the TGx-HDACi biomarker in classifying external compounds, TempO-Seq gene expression profiles of an additional 11 compounds were classified using the biomarker in a probability analysis (Fig. 2B), PCA, hierarchical clustering (Fig. 3), and the Running Fisher test (Fig. 4). All compounds classified as expected using the probability analysis. In the PCA and hierarchical clustering, all 11 compounds clustered with the correct group within the reference compound set. Entinostat, a selective inhibitor of Class I HDACs, clustered with the two class I inhibitors in the reference set, tacedinaline and mocetinostat, in the PCA and the three compounds also formed a separate branch within the HDACi branch in hierarchical clustering. All 7 non-HDACi and 4 HDACi were correctly classified using the Running Fisher test with a –Log10(p-value) cut-off of 15.

The overall classification accuracy of the TGx-HDACi biomarker in external validation was 100%. Table 3 summarizes the results of the TGx-HDACi analysis of the 11 external validation compounds.

DISCUSSION

MOA-specific transcriptomic biomarkers provide a practical approach to efficiently identify MIE and KE perturbations from high-content gene expression data. The availability of diverse transcriptomic biomarkers will enable rapid screening of gene expression profiles for multiple MOAs concurrently. Currently, there are no transcriptomic biomarkers of HDACi that are adequate for applications in chemical screening after short-term exposures *in vitro*. Herein, we developed an 81-gene biomarker of HDACi that can be measured after 4-hour exposures in TK6 cells and assessed in parallel with the TGx-DDI transcriptomic biomarker for genotoxicity.

The TGx-HDACi biomarker was derived from TempO-Seq whole transcriptome gene expression profiles of TK6 human lymphoblastoid cells exposed for 4 hours to a reference compound set consisting of 10 HDACi and 10 non-HDACi compounds. The classification capability of TGx-HDACi was first assessed by classifying the reference set, followed by an external validation set consisting of four HDACi and seven non-HDACi compounds. Four different statistical analyses, probability analysis, PCA, hierarchical clustering, and the Running Fisher test, were used to assess the classification capabilities. The biomarker demonstrated 100% accuracy in classifying the 20 reference compounds and the 11 external validation compounds as HDACi or non-HDACi in all analyses. Notably, three of the seven non-HDACi validation compounds were histone modulators: garcinol, a histone acetyltransferase inhibitor, GSK-J4, a histone demethylase inhibitor, and 3-deazaneplanocin A (DZNep), a histone methyltransferase inhibitor (Balasubramanyam et al. 2004; Girard et al. 2014; Li et al. 2015a, b; Lochmann et al. 2018). The external validation results suggest that the biomarker is capable of distinguishing HDACi from inhibitors of other histone modulating enzymes. Overall, the TGx-HDACi biomarker demonstrated a robust classification performance with a promising specificity toward HDACi in TK6 cells.

We applied four different statistical analyses to perform chemical classifications using TGx-HDACi (Table 3). The use of probability analysis, PCA, and hierarchical clustering was

adapted from the three-pronged classification approach employed by Li et al. (2017) for TGx-DDI; the results of the three analyses were combined to make an overall chemical classification, in which a negative call was made only when all three analyses were negative, while one positive analysis led to an overall positive call (Li et al. 2017, 2019). This approach provides sensitivity to the biomarker assay and conservative negative calls of toxicity. The three-pronged approach is useful for assessing individual compounds rather than screening a large dataset. In contrast, the Running Fisher test enables rapid screening and ranking of chemicals within large databases such as Illumina BaseSpace Correlation Engine with existing transcriptomic data (Kupershmidt et al. 2010; Corton et al. 2018; 2019). Concordant classifications made using the two approaches suggest that the two methods can be combined or applied separately to accurately classify chemicals in the TGx-HDACi analysis.

In the PCA of the reference and validation compounds (Fig. 3; left panel), three HDACi compounds, mocetinostat, entinostat, and tacedinaline, formed a distinct cluster away from the remaining HDACi. The three HDACi also formed a separate branch within the HDACi cluster in hierarchical clustering (Fig. 3; right panel). These three compounds are all benzamides that are selective inhibitors of class I HDACs (HDAC1, 2, 3, and 8), while the remaining HDACi in the reference and validation sets are pan-HDACi that inhibit classes I, II, and IV enzymes (Kraker et al. 2003; Agudelo et al. 2016; Surolia and Bates 2018). The differences between class I HDACi and pan-HDACi can be observed in the heatmaps of TGx-HDACi, in which the three class I HDACi induce expression patterns that are visibly different across the 81 genes compared to the rest of the HDACi set (Fig. 2). These results suggest that selective inhibitors of different classes of HDAC can be distinguished from each other by gene expression profiles in TK6 cells and that it may be possible to derive transcriptomic signatures for selective HDACi. The analysis also demonstrates the added value of the clustering approaches to classify chemicals, which can provide more insight into chemical similarities to understand the MOA. We note that TGx-HDACi addresses inhibitors of the classical, Zn^{2+-}dependent human HDACs in classes I, II, and IV but not inhibitors of the NAD^{+}-dependent class III HDACs (i.e., sirtuins). Future work is needed to develop biomarkers of class III HDAC inhibitors.

Although HDACs were initially known for deacetylation of lysine residues in histone tails, an increasing number of non-histone targets of deacetylation by HDACs are being elucidated (e.g., p53 (Brooks and Gu 2011)) and a broader range of activities beyond the epigenetic regulation of transcription have been associated with HDACs (Wright and Menick 2016; Narita et al. 2019). Acetylation and deacetylation of non-histone proteins by HATs and HDACs, respectively, regulate the stability and function of proteins involved in diverse cellular processes (e.g., DNA damage response (Thurn et al. 2013); mRNA elongation and splicing (Greer et al. 2015; Rahhal and Seto 2019); microtubule stabilization (Janke and Montagnac 2017)). Therefore, the transcriptomic changes observed under HDACi exposures may be due to inhibited deacetylation of not only histones but many other proteins, and perturbations of diverse pathways. Perhaps unsurprisingly, an enrichment analysis of the 81 genes in Ingenuity Pathway Analysis of the TGx-HDACi biomarker genes did not reveal any significant enrichment of pathways, processes or upstream regulators (data not shown).

There is a considerable overlap between the reference compound sets of TGx-DDI and TGx-HDACi biomarker, as the latter was constructed by leveraging the 28 reference compounds used in the initial TGx-DDI study; all 10 non-HDACi and three of the HDACi reference compounds were shared in the development of the two biomarkers (Li et al. 2015a, b). TGx-DDI detects gene expression changes in response to agents that directly induce DNA damage, such as alkylators (e.g., methyl methanesulfonate) and topoisomerase inhibitors (e.g., campthothecin); four HDACi were included as non-DDI reference compounds. The non-HDACi reference set contains six DDI compounds that were part of the DDI reference set used to develop TGx-DDI. Consequently, there are only two genes, *COIL* and *E2F8,* are shared by the two biomarkers. Thus far, analysis of the two biomarkers in the same gene expression profile yields positive results that are mutually exclusive of one another.

Pleiotropic activities are characteristic of many HDACi. Genotoxicity has been identified as an off-target effect of a number of HDACi compounds. For example, TSA and vorinostat, both hydroxamates, are mutagenic in the Ames test and clastogenic in mammalian cells *in vitro* and *in vivo* through indeterminate mechanisms (Olaharski et al. 2006; Kerr et al. 2010; Lee et al. 2010; Shen and Kozikowski 2016). Of note, TSA was a non-DDI reference compound for TGx-DDI. HDACi compounds are suspected to induce genotoxicity through indirect mechanisms such as the induction of reactive oxygen species (ROS) and oxidative stress, and inhibition of DNA repair (Zhang et al. 2007; Petruccelli et al. 2011; Li et al. 2015a, b).

The TGx-DDI biomarker is enriched in p53-associated genes and a positive call is consistent with p53 activation (Corton et al. 2019). The lack of overlap in the induction of the TGx-HDACi and TGx-DDI biomarkers, despite the reported genotoxicity of many HDACi compounds, could be due to a combination of the indirect mechanisms leading to DNA damage (e.g., induction of ROS), the concentration and exposure duration required for HDACi to cause DNA damage (may require exposures longer than 4 h), and/or the perturbation of p53-related transcriptional responses to DNA damage via HDACi. Thus, when assessing chemicals using these two transcriptomic biomarkers, the possibility of a positive HDACi outcome suppressing the TGx-DDI biomarker response should be considered; pairing these biomarkers would clearly enrich mechanistic understanding of chemical effects.

Because HDACs are involved in the regulation of p53-related signaling and transcriptional activities, inhibiting HDACs interferes with p53 responses and thereby prevents proper DNA damage signaling and repair (Hamms and Chen 2007; Roos and Krumm 2016). For example, HDACi has been observed to attenuate the activation of Ataxia-telangiectasia mutated (ATM), an upstream regulator of p53 in DNA damage response, and to modulate p53-regulated responses to genotoxic stress such as apoptosis and DNA repair (Zhang et al. 2007; Jang et al. 2010; Brochier et al. 2013; Thurn et al. 2013). However, when we compared TGx-HDACi to a list of 350 p53-regulated genes curated by Fischer (2017), only three genes, *CPEB4*, *YRK3*, and *FAS,* were present in both gene sets (Fischer 2017); based on the 81 genes of TGx-HDACi, the impact of HDACi on p53 responses cannot be determined. Moreover, TGx-HDACi is just a small subset of genes that are affected by HDACi. An analysis of the whole transcriptome profiles of HDACi produced herein

would improve the understanding of the impact of HDACi on p53 responses. In addition, given that perturbations of various pathways are downstream events of HDACi-induced hyperacetylation of histones, exposures longer than 4 h may be required to observe the effects of HDACi on p53 responses.

Previous studies by Rempel et al. (2015), Dreser et al. (2015), and Yeakley et al. (2017) investigated transcriptomic responses to HDACi. Rempel et al. and Dreser et al. used human pluripotent stem cells to develop an 8-gene classifier to distinguish HDACi from mercurial compounds and to observe HDACi-induced perturbations in 35 genes related to neural crest development, respectively (Dreser et al. 2015; Rempel et al. 2015). Unsurprisingly, none of the genes analyzed in these studies overlap with TGx-HDACi as they were identified and selected based on very different criteria from the TGx-HDACi genes. In contrast, 21 overlapping genes were identified in a list of 330 TSA-responsive genes generated by Yeakley et al.; the differential expression of these 330 genes measured by TempO-Seq were consistent across 5 cell types (MCF-7, PC-3, undifferentiated HL-60, and 2 differentiation states of HL-60) after 6 h of exposure (Yeakley et al. 2017). TGx-HDACi was one of multiple candidates for a potential HDACi biomarker, which indicates there may be additional genes in the Yeakley et al. gene set that can contribute to building an HDACi classifier. A biomarker reference compound set that includes data from other cell lines could possibly yield a biomarker of HDACi that can be measured in multiple cell lines.

The concentration optimization strategy originally designed and applied by Li et al. (2015a, b) to develop the TGx-DDI biomarker was modified to select one concentration for each HDACi for whole transcriptome profiling and signature derivation. The three HDACi indicator genes, *RGN1, NEU1,* and *GPR183,* were chosen based on DNA microarray profiles of four HDACi produced in the aforementioned study. While *GPR183* was among the 81 genes of TGx-HDACi, *RGN1* and *NEU1* were excluded. While *GPR183* was consistently down-regulated by all HDACi, the responses in *RGN1* and *NEU1* varied between class I-selective HDACi and pan-HDACi. It is possible that when all 20 reference compounds were considered in the NSC method and cross-validation, the centroids of the two genes were below the final threshold and did not sufficiently contribute to the signature. The concentration-response analysis of three indicator genes by qPCR was nonetheless effective in identifying concentrations that were suitable for biomarker development, as demonstrated by the HDACi signature derived herein.

While the TGx-HDACi biomarker and other transcriptomic biomarkers can facilitate efficient analyses of high-content transcriptomic data, applications could be limited by several factors. The TGx-HDACi biomarker is currently limited to TK6 cells and the TempO-Seq gene expression platform; reliable classifications in other cell lines and different platforms would require further validation, similar to the extensive validation experiments performed for the TGx-DDI biomarker (Li et al. 2019). Furthermore, only one concentration of each validation compound was tested at one time point in this study. In a chemical assessment setting, multiple concentrations and exposure durations should be tested to enable different biomarker assay applications (e.g., TGx-HDACi and TGx-DDI might be detected at different concentrations and times) and quantitative analyses. Future studies will investigate the utility of the two biomarkers in an integrated approach to testing and

assessment, complementing predictive tools such as Adverse Outcome Pathways. Case studies will be performed to demonstrate and determine the optimal approach to integrating these transcriptomic biomarkers in chemical assessment.

In summary, we developed an 81-gene transcriptomic biomarker of HDACi to detect chemicals that operate through this MIE using gene expression profiles of TK6 cells. The biomarker accurately classifies HDACi in cross-validation and external validation experiments, in addition to distinguishing HDACi from other epigenotoxic mechanisms. Both the TGx-DDI and TGx-HDACi biomarkers can be analyzed concurrently in TK6 cells after 4-hour exposures. These biomarkers can be implemented as first tier tests in integrated testing and assessment of chemicals, or in MOA analyses, to efficiently identify the MIE of toxicants.

(Rempel et al. 2015; Dreser et al. 2015)

Supplementary Material

Refer to Web version on PubMed Central for supplementary material.

ACKNOWLEDGEMENTS

This project was supported by funds from Health Canada's Genomics Research and Development Initiative awarded to CLY. Stipend support for EC was also provided through the Research in Environmental and Analytical Chemistry and Toxicology (REACT) program funded under the Natural Science and Engineering Council of Canada (NSERC)'s Collaborative Research and Training (CREATE) Program. The information in this document has subjected to review by the Center for Computational Toxicology and Exposure of the US EPA and approved for publication. Approval does not signify that the contents reflect the views of the Agency, nor does mention of trade names or commercial products constitute endorsement or recommendation for use. We would like to thank Rémi Gagné and Dr. Matthew Meier (Health Canada) for their support in data processing and the reviewers Drs. Daniel Desaulniers, Mike Wade (Health Canada), and Brian Chorley (US EPA) for their input on the manuscript.

ABBREVIATIONS

DDI	DNA damage-inducing
HAT	Histone acetyltransferase
HDACi	Histone deacetylase inhibitor
KE	Key event
MIE	Molecular initiating event
MOA	Mode of action
NSC	Nearest shrunken centroid
PCA	Principal component analysis
PTM	Post-translational modification
TempO-seq	Templated Oligo-sequencing
TGx	Toxicogenomics

REFERENCES

Agudelo M, Figueroa G, Parira T, et al. (2016) Profile of Class I Histone Deacetylases (HDAC) by Human Dendritic Cells after Alcohol Consumption and In Vitro Alcohol Treatment and Their Implication in Oxidative Stress: Role of HDAC Inhibitors Trichostatin A and Mocetinostat. PLOSone 11:e0156421.

Audia J, Campbell R (2016) Histone Modifications and Cancer. Cold Spring Harb Perspect Biol 8:a019521. [PubMed: 27037415]

Balasubramanyam K, Altaf M, Varier RA, et al. (2004) Polyisoprenylated Benzophenone, Garcinol, a Natural Histone Acetyltransferase Inhibitor, Represses Chromatin Transcription and Alters Global Gene Expression. J Biol Chem 279:33716–33726. [PubMed: 15155757]

Biswas M, Voltz K, Smith J, Langowski J (2011) Role of Histone Tails in Structural Stability of the Nucleosome. PLoS Comput Biol 7:e1002279. 10.1371/journal.pcbi.1002279 [PubMed: 22207822]

Bose P, Dai Y, Grant S (2014) Histone deacetylase inhibitor (HDACI) mechanisms of action: Emerging insights. Pharmacol Ther 143:323–336. [PubMed: 24769080]

Brochier C, Dennis G, Rivieccio M, et al. (2013) Specific acetylation of p53 by HDAC inhibition prevents DNA damage-induced apoptosis in neurons. The Journal of Neuroscience 33:8621–8632. [PubMed: 23678107]

Brooks CL, Gu W (2011) The impact of acetylation and deacetylation on the p53 pathway. Protein Cell 2:456–462. [PubMed: 21748595]

Chang PV, Hao L, Offermanns S, Medzhitov R (2014) The microbial metabolite butyrate regulates intestinal macrophage function via histone deacetylase inhibition. Proc Natl Acad Sci USA 111:2247–2252. 10.1073/pnas.1322269111 [PubMed: 24390544]

Cho E, Buick JK, Williams A, et al. (2019) Assessment of the performance of the TGx-DDI biomarker to detect DNA damage-inducing agents using quantitative RT-PCR in TK6 cells. Environ Mol Mutagen 60:122–133. 10.1002/em.22257 [PubMed: 30488505]

Corton JC, Williams A, Yauk CL (2018) Using a gene expression biomarker to identify DNA damage-inducing agents in microarray profiles. Environ Mol Mutagen 59:772–784. 10.1002/em.22243 [PubMed: 30329178]

Corton JC, Witt KL, Yauk CL (2019) Identification of p53 Activators in a Human Microarray Compendium. Chem Res Toxicol 32:1748–1759. 10.1021/acs.chemrestox.9b00052 [PubMed: 31397557]

Damaskos C, Valsami S, Kontos M, et al. (2017) Histone Deacetylase Inhibitors: An Attractive Therapeutic Strategy Against Breast Cancer. Anticancer Res 37:35–46. [PubMed: 28011471]

Dreser N, Zimmer B, Dietz C, et al. (2015) Grouping of histone deacetylase inhibitors and other toxicants disturbing neural crest migration by transcriptional profiling. Neurotoxicology 50:56–70. 10.1016/j.neuro.2015.07.008 [PubMed: 26238599]

Fischer M (2017) Census and evaluation of p53 target genes. Oncogene 36:3943–3956. 10.1038/onc.2016.502 [PubMed: 28288132]

Gallinari P, Di Marco S, Jones P, Pallaoro M, Steinkuhler D (2007) HDACs, histone deacetylation and gene transcription: from molecular biology to cancer therapeutics. Cell Research 17:195–211. [PubMed: 17325692]

Girard N, Bazille C, Lhuissier E, et al. (2014) 3-Deazaneplanocin A (DZNep), an Inhibitor of the Histone Methyltransferase EZH2, Induces Apoptosis and Reduces Cell Migration in Chondrosarcoma Cells. PLoS One 9:e98176. [PubMed: 24852755]

Greer CB, Tanaka Y, Kim Y, J., et al. (2015) Histone Deacetylases Positively Regulate Transcription through the Elongation Machinery. Cell Rep 13:1444–1455. 10.1016/j.celrep.2015.10.013 [PubMed: 26549458]

Hamms KL, Chen X (2007) Histone Deacetylase 2 Modulates p53 Transcriptional Activities through Regulation of p53-DNA Binding Activity. Cancer Res 67:3145–3152. [PubMed: 17409421]

Hastie T, Tibshirani R, Friedman J (2001) Cross-Validation. The Elements of Statistical Learning: Data Mining, Inference, and Prediction Springer, New York, pp 241–249

Jang ER, Choi JD, Park MA, Jeong G, Cho H, Lee J- (2010) ATM modulates transcription in response to histone deacetylase inhibition as part of its DNA damage response. Exp Mol Med 42:195–204. [PubMed: 20164679]

Janke C, Montagnac G (2017) Causes and Consequences of Microtubule Acetylation. Curr Biol 27:R1287–R1292. [PubMed: 29207274]

Kerr JS, Galloway S, Lagrutta A, et al. (2010) Nonclinical Safety Assessment of the Histone Deacetylase Inhibitor Vorinostat. Int J Toxicol 29:3–19. 10.1177/1091581809352111 [PubMed: 19903873]

Kraker AJ, Mizzen CA, Harti JM, Allis CD, Merriman RL (2003) Modulation of Histone Acetylation by [4-(Acetylamino)-N-(2-Amino-phenyl) Benzamide] in HCT-8 Colon Carcinoma. Mol Cancer Ther 2:401–408. [PubMed: 12700284]

Kupershmidt I, Su QJ, Grewal A, et al. (2010) Ontology-Based Meta-Analysis of Global Collections of High-Throughput Public Data. PLoS One 5:e13066. 10.1371/journal.pone.0013066 [PubMed: 20927376]

Law C, Chen Y, Shi W, Smyth G (2014) voom: precision weights unlock linear model analysis tools for RNA-seq read counts. Genome Biol 15:R29. [PubMed: 24485249]

Lee JH, Choy ML, Ngo L, Foster SS, Marks PA (2010) Histone deactylase inhibitor induces DNA damage, which normal but not transformed cells can repair. Proc Natl Acad Sci USA 107:14639–14644. [PubMed: 20679231]

Li HH, Chen R, Hyduke DR, et al. (2017) Development and validation of a high-throughput transcriptomic biomarker to address 21st century genetic toxicology needs. Proc Natl Acad Sci USA 114:E10881–E10889. 10.1073/pnas.1714109114 [PubMed: 29203651]

Li HH, Hyduke DR, Chen R, et al. (2015a) Development of a Toxicogenomics Signature for Genotoxicity Using a Dose-Optimization and Informatics Strategy in Human Cells. Environ Mol Mutagen 56:505–519. 10.1002/em.21941 [PubMed: 25733355]

Li HH, Yauk CL, Chen RX, et al. (2019) TGx-DDI, a Transcriptomic Biomarker for Genotoxicity Hazard Assessment of Pharmaceuticals and Environmental Chemicals. Front Big Data 2:36. 10.3389/fdata.2019.00036 [PubMed: 33693359]

Li L, Sun Y, Liu J, et al. (2015b) Histone deacetylase inhibitor sodium butyrate suppresses DNA double strand break repair induced by etoposide more effectively in MCF-7 cells than in HEK293 cells. BMC Biochem 16: 10.1186/s12858-014-0030-5

Lochmann TL, Powell KM, Ham J, et al. (2018) Targeted inhibition of histone H3K27 demethylation is effective in high-risk neuroblastoma. Sci Trans Med 10:eaao4680.

Millard CJ, Watson PJ, Fairall L, Schwabe JW (2017) Targeting Class I Histone Deacetylases in a “Complex” Environment. Trends Pharmacol Sci 38:363–377. [PubMed: 28139258]

Morris MJ, Monteggia LM (2014) Unique functional roles for class I and class II histone deacetylases in central nervous system development and function. Int J Dev Neuro 31:370–381. 10.1016/j.ijdevneu.2013.02.005

Narita T, Weinert B, Choudhary C (2019) Functions and mechanisms of non-histone protein acetylation. Nature Rev Mol Cell Biol 20:156–174. [PubMed: 30467427]

Olaharski A, Ji Z, Woo J, et al. (2006) The histone deacetylase inhibitor trichostatin A has genotoxic effects in human lymphoblasts in vitro. Toxicol Sci 93:341–347. [PubMed: 16857700]

Park SY, Kim JS (2020) A short guide to histone deacetylases including recent progress on class II enzymes. Exp Mol Med 52:204–212. [PubMed: 32071378]

Petruccelli LA, Dupere-Richier D, Pettersson F, Retrouvey H, Skoulikas S, Miller WH Jr. (2011) Vorinostat Induces Reactive Oxygen Species and DNA Damage in Acute Myeloid Leukemia Cells. PLoS One 6:e20987. [PubMed: 21695163]

Rahhal R, Seto E (2019) Emerging roles of histone modifications and HDACs in RNA splicing. Nucleic Acids Res 47:4911–4926. 10.1093/nar/gkz292 [PubMed: 31162605]

Rajan A, Shi H, Xue B (2018) Class I and II Histone Deacetylase Inhibitors Differentially Regulate Thermogenic Gene Expression in Brown Adipocytes. Sci Rep 8:13072. 10.1038/s41598-018-31560-w [PubMed: 30166563]

Rempel E, Hoelting L, Waldmann T, et al (2015) A transcriptome-based classifier to identify developmental toxicants by stem cell testing: design, validation and optimization for histone deacetylase inhibitors. Arch Toxicol 89:1599–1618. [PubMed: 26272509]

Roos WR, Krumm A (2016) The multifaceted influence of histone deacetylases on DNA damage signalling and DNA repair. Nucleic Acids Res 44:10017–10030. 10.1093/nar/gkw922 [PubMed: 27738139]

Seto E, Yoshida M (2013) Erasers of Histone Acetylation: The Histone Deacetylase Enzymes. Cold Spring Harb Perspect Biol 6:a018713. 10.1101/cshperspect.a018713

Shen S, Kozikowski AP (2016) Why Hydroxamates May Not Be the Best Histone Deacetylase Inhibitors—What Some May Have Forgotten or Would Rather Forget? Chem Med Chem 11:15–21. 10.1002/cmdc.201500486 [PubMed: 26603496]

Surolia I, Bates S (2018) Entinostat finds a path: A new study elucidates effects of the histone deacetylase inhibitor on the immune system. Cancer 124:4657–4666. [PubMed: 30423192]

Thurn K, Thomas S, Raha P, Qureshi I, Munster P (2013) Histone deacetylase regulation of ATM-mediated DNA damage signaling. Molecular Cancer Therapeutics 12:2078–2087. [PubMed: 23939379]

Tibshirani R, Hastie T, Balasubramanian N, Chu G (2002) Diagnosis of multiple cancer types by shrunken centroids of gene expression. Proc Natl Acad Sci USA 99:6567–6572. [PubMed: 12011421]

Vandesompele J, De Preter K, Pattyn F, et al. (2002) Accurate normalization of real-time quantitative RT-PCR data by geometric averaging of multiple internal control genes. Genome Biol 3:research0034.1-research0034.11.

Ventrelli S, Berger A, Bocker A, et al. (2013) Resveratrol as a Pan-HDAC Inhibitor Alters the Acetylation Status of Jistone Proteins in Human-Derived Hepatoblastoma Cells. PLoS One 8:e73097. 10.1371/journal.pone.0073097 [PubMed: 24023672]

Wade MG, Kawata A, Williams A, Yauk CL (2008) Methoxyacetic acid-induced spermatocyte death is associated with histone hyperacetylation in rats. Biol Reprod 78:822–831. [PubMed: 18199887]

Wright LH, Menick DR (2016) A class of their own: exploring the nondeacetylase roles of class IIa HDACs in cardiovascular disease. Am J Physiol Heart Circ Physiol 311:H199–H206. [PubMed: 27208161]

Yeakley J, Shepard P, Goyena D, VanSteenhouse H, McComb J, Seligmann B (2017) A trichostatin A expression signature identified by TempO-Seq targeted whole transcriptome profiling. PLoS One 12:e0178302. [PubMed: 28542535]

Zhang L, Zhang J, Jiang Q, Zhang L, Song W (2018) Zinc binding groups for histone deacetylase inhibitors. J Enzyme Inhib Med Chem 33:714–721. 10.1080/14756366.2017.1417274 [PubMed: 29616828]

Zhang Y, Carr T, Dimtchev A, Zaer N, Dritschilo A, Jung M (2007) Attenuated DNA Damage Repair by Trichostatin A through BRCA1 Suppression. Radiat Res 168:115–124. [PubMed: 17722998]

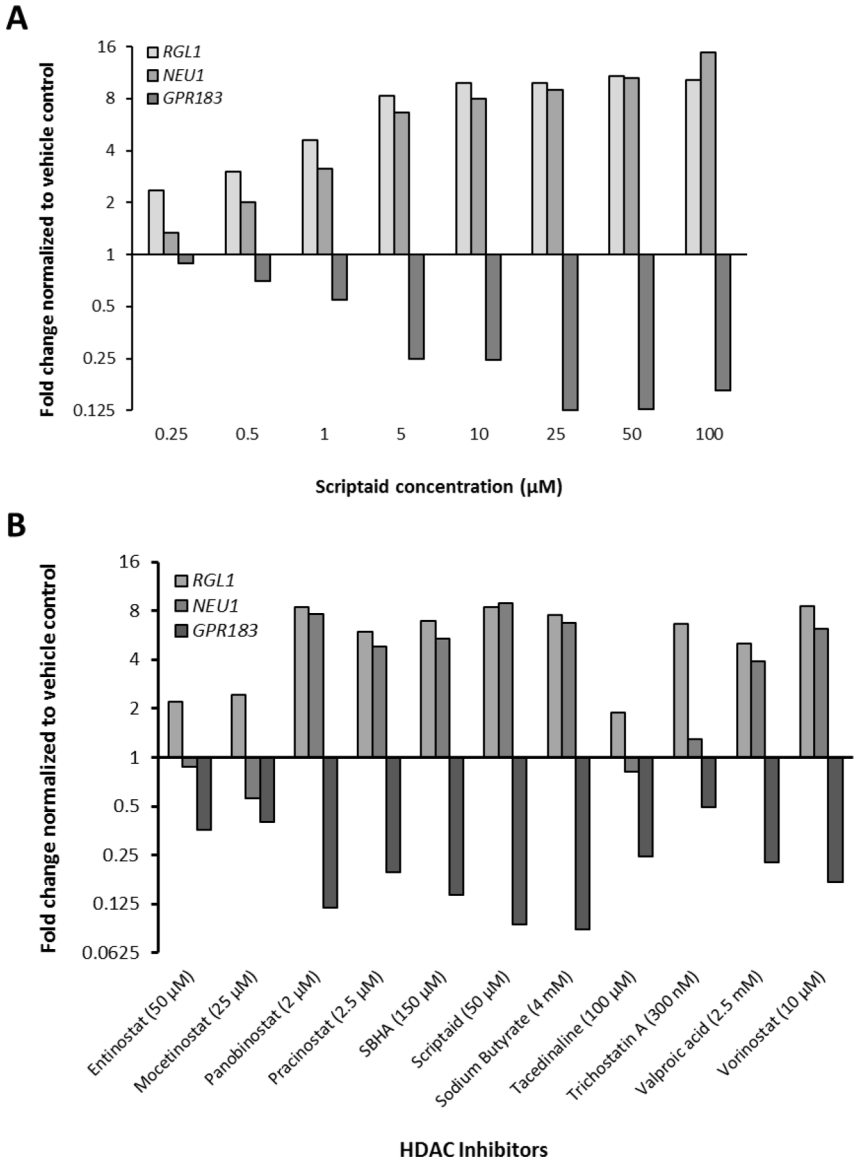

Fig. 1.

Quantitative RT-PCR measurements of the three HDACi indicator genes, *RGL1, NEU1,* and *GPR183* **A:** The concentration-response of the three indicator genes in TK6 cells exposed to scriptaid, a reference HDACi, for 4 hours. The bars represent the averaged fold change of two technical replicates normalized to the vehicle control. Fifty μM was selected for whole transcriptome profiling. The expression profiles of all tested compounds are included in Supplementary Fig. S1 **B:** The fold changes in the three indicator genes measured in TK6 cells exposed to HDACi at the concentrations selected for whole transcriptome profiling.

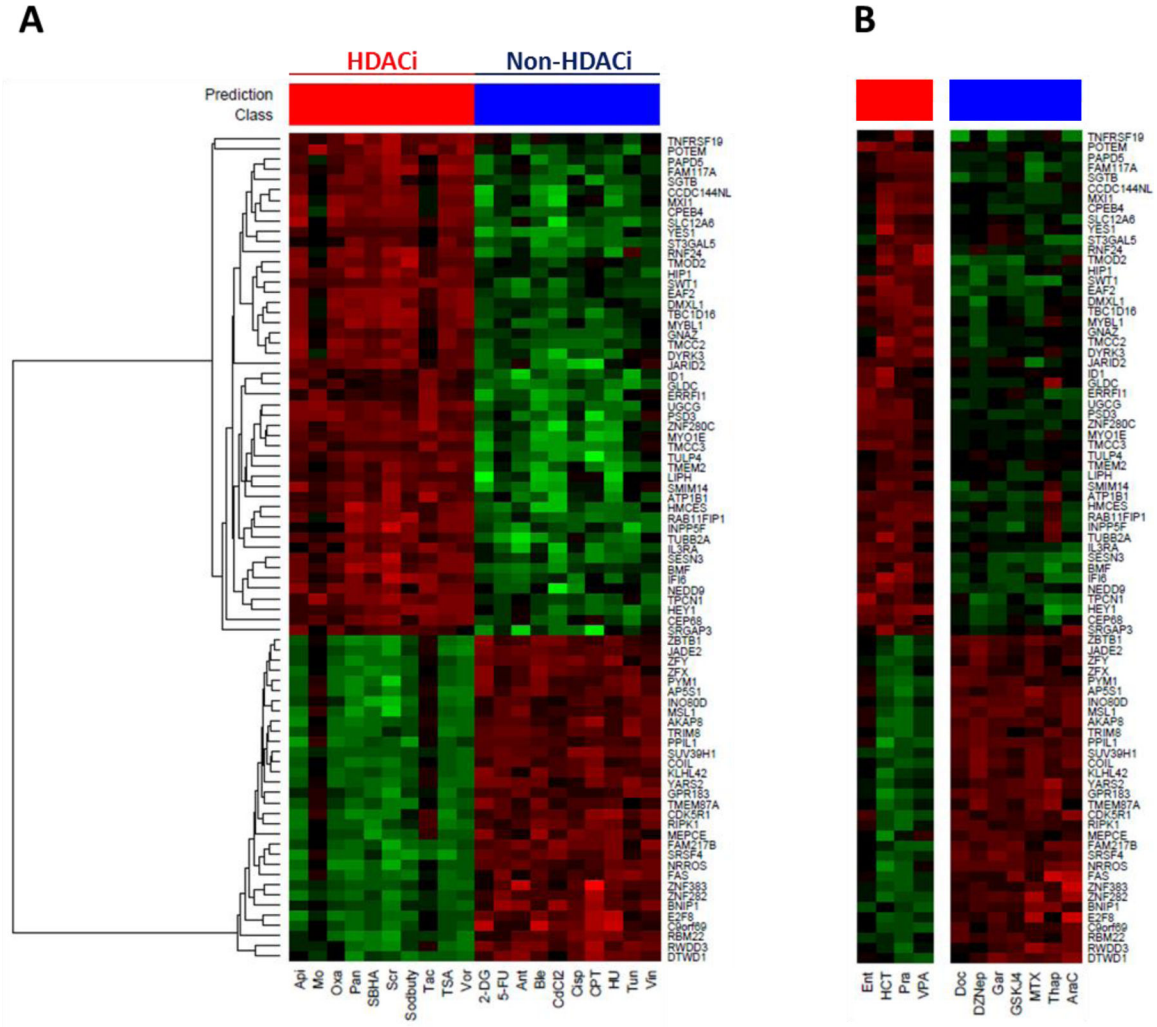

Fig. 2.

Heatmap of the TGx-HDACi biomarker genes in TK6 cells exposed to the reference **(A)** or validation **(B)** compounds for 4 hours. The gene expression profiles have been averaged across three replicates, except for Tac, Pra, and MTX (n=2). The biomarker genes are on the Y-axis and the chemicals are on the X-axis. Red indicates gene up-regulation and green indicates gene down-regulation in the heat maps. The bars above the heat maps show the class of the chemical and the prediction made by the biomarker in the probability analysis – HDACi in red and non-HDACi in blue.

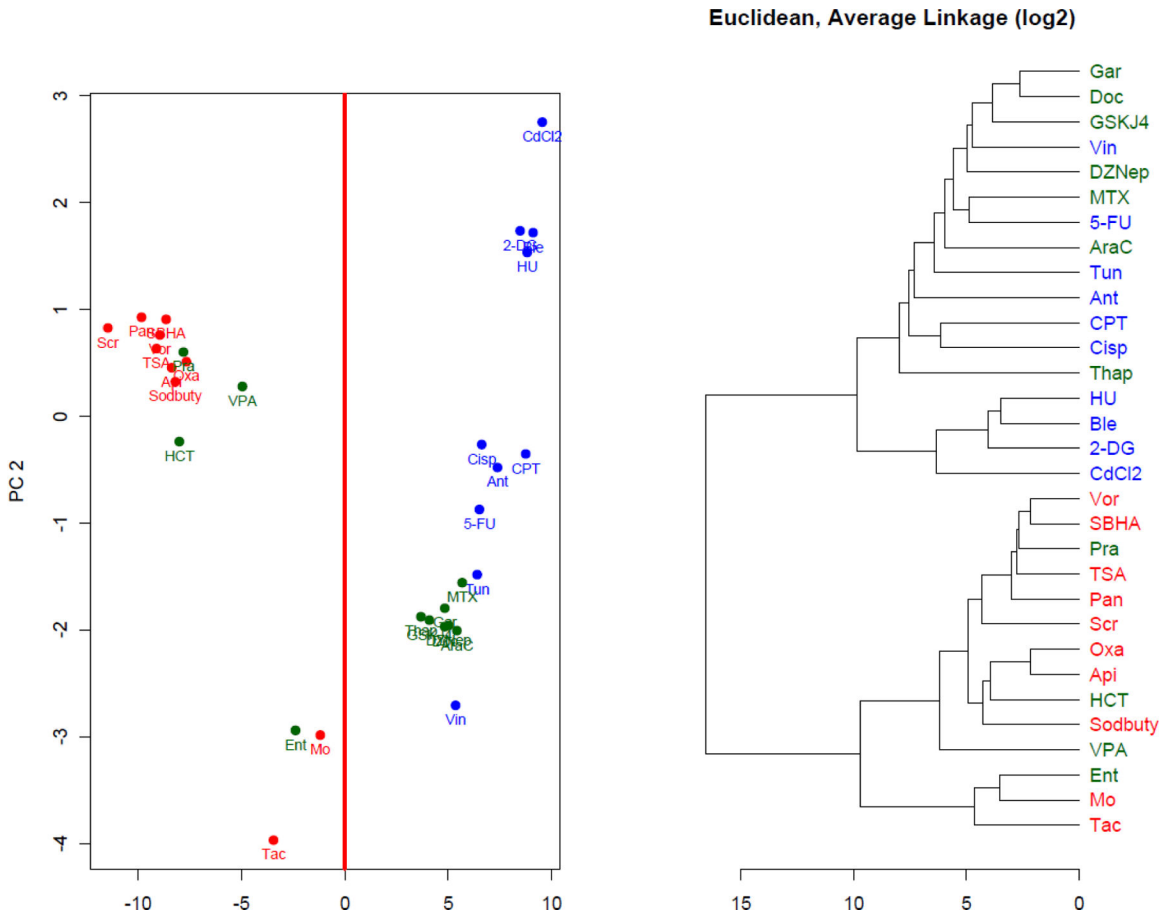

Fig. 3.

Principal component analysis (left) and 2-dimensional hierarchical clustering (right) of the TGx-HDACi biomarker genes by TempO-Seq analysis following exposure to the 20 reference and 11 external compounds for 4 hours. The data represent the average across three replicates, except for Tac, Pra, and MTX (n=2). Red font indicates reference HDACi and blue font indicates non-HDACi reference compounds. Green font indicates external validation compounds.

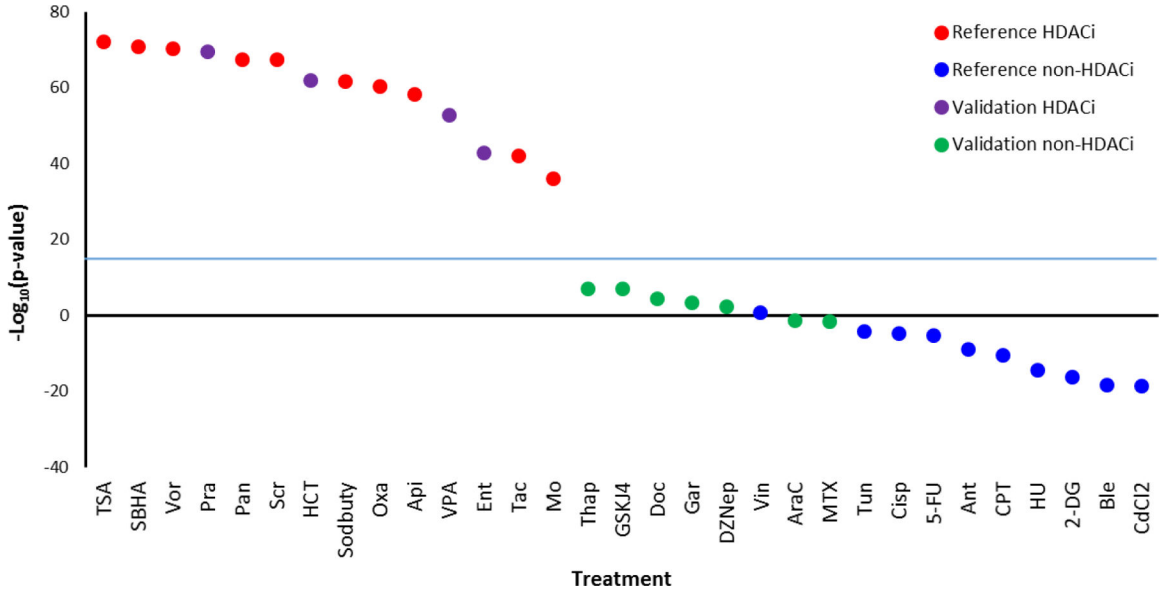

Fig. 4.

The Running Fisher test results for the 20 reference compounds and 11 external validation compounds using the TGx-HDACi biomarker expression profile. The red dots indicate HDACi and blue dots indicate non-HDACi reference compounds. Purple and green dots represent the HDACi and non-HDACi external validation compounds, respectively. Chemicals are ranked by $-Log_{10}$(P-value) from the highest on the left to the lowest on the right. A cut-off of 15 was derived from the reference set for use in classification. Chemicals above the cut-off are classified as HDACi and ones below are classified as non-HDACi.

Table 1.

Reference set for HDACi transcriptomic biomarker derivation.

Mode of Action	Chemical	Abbreviation	Solvent	Tested Concentration Range	Selected Concentration	Manufacturer/ CAS #
Pan HDACi *	Apicidin	Api	DMSO	0.25 – 4 μg/ml ≠	1 μg/ml	Sigma Aldrich/ 183506–66-3
Class I HDACi	Mocetinostat	Mo	DMSO	0.25 – 50 μM	25 μM	Cayman Chemical/ 726169–73-9
Pan HDACi	Oxamflatin	Oxa	DMSO	0.25 – 4 μM ≠	1 μM	Sigma Aldrich/ 151720–43-3
Pan HDACi	Panobinostat	Pan	DMSO	0.025 – 100 μM	2 μM	Focus BioSciences/ 404950–80-7
Pan HDACi	Scriptaid	Scr	DMSO	0.25 – 100 μM	50 μM	Tocris Bioscience/ 287383–59
Pan HDACi	Sodium butyrate	SodButy	H_2O	0.05 – 10 mM	4 mM	Sigma Aldrich/ 156–54-7
Pan HDACi	Suberohydroxamic acid	SBHA	DMSO	15.63 – 1000 μM	150 μM	Sigma Aldrich/ 38937–66-5
Class I HDACi	Tacedinaline	Tac	DMSO	0.3125 – 100 μM	100 μM	Sigma Aldrich/ 112522–64-2
Pan HDACi	Trichostatin A	TSA	DMSO	5 – 300 nM	300 nM	Active Motif Inc./ 58880–19-6
Pan HDACi	Vorinostat	Vor	DMSO	0.025 – 100 μM	10 μM	StressMarq BioSciences/ 149647–78-9
Glycolysis inhibitor	2-Deoxyglucose	2-DG	H_2O	0.16 – 20 μM ≠	20 μM	Sigma Aldrich/ 154–17-6
DNA antimetabolite	5-Fluorouracil	5-FU	DMSO	6.25 – 50 μg/ml ≠	25 μg/ml	Sigma Aldrich/ 51–21-8
Electron transport chain uncoupler	Antimycin A	Ant	DMSO	25 – 200 μM ≠	100 μM	Sigma Aldrich/ 1397–94-0
Clastogen	Bleomycin	Ble	H_2O	5 – 40 μg/ml ≠	10 μg/ml	Sigma Aldrich/ 11056–06-7
Oxidative stressor/ DNA repair inhibitor	Cadmium chloride	$CdCl_2$	H_2O	50 – 800 μM ≠	50 μM	J. T. Baker/ 10108–64-2
DNA alkylator/cross-linker	Cisplatin	Cisp	DMSO	10 – 80 μM ≠	80 μM	Sigma Aldrich/ 15663–27-1
Topoisomerase inhibitor	Camptothecin	CPT	DMSO	62.5 – 500 nM ≠	125 nM	Sigma Aldrich/ 7689–03-4
DNA antimetabolite	Hydroxyurea	HU	H_2O	0.25 – 1 mM ≠	0.5 mM	Sigma Aldrich/ 127–07-1
Endoplasmic reticulum modulator	Tunicamycin	Tun	DMSO	1.25 – 10 μg/ml ≠	2.5 μg/ml	Sigma Aldrich/ 11089–65-9
Tubulin polymerization inhibitor	Vinblastine	Vin	DMSO	50 – 800 ng/ml ≠	200 ng/ml	Sigma Aldrich/ 865–21-4

* Pan HDACi indicates non-selective HDACi that inhibit classical HDACs in classes I, II, and IV.

≠ Concentration range tested by Li et al. (2015a, b) in TK6 cells; range finding experiments for these chemicals were not repeated in this study.

Table 2.

External validation compounds

Mode of Action	Chemical	Abbreviation	Solvent	Tested Concentration Range	Selected Concentration	Manufacturer/ CAS #
Class I HDACi	Entinostat	Ent	DMSO	0.006 – 100 μM	50 μM	ApexBio/ 209783–80-2
Pan-HDACi	HC Toxin	HCT	MeOH	5 – 80 ng/ml[≠]	20 ng/ml	Sigma Aldrich/ 209783–80-2
Pan-HDACi	Pracinostat	Pra	DMSO	0.0625 – 100 μM	2 μM	ApexBio/ 929016–96-6
Pan-HDACi	Valproic acid	VPA	H_2O	0.001 – 10 mM	2.5 mM	StressMarq BioSciences/ 1069–66-5
Nucleotide analogue	Arabinofuranosyl cytidine	AraC	DMSO	12.5 – 100 μM	25 μM	Toronto Research Chemicals/ 147–94-4
Tublin Inhibitor	Docetaxel	Doc	DMSO	12.5 – 100 nM	50 nM	Cayman Chemical/ 114977–28-5
Antifolate	Methotrexate	MTX	DMSO	0.05 – 1 μM	250 nM	Cayman Chemical/ 59–05-2
ER Ca2+ ATPase inhibitor	Thapsigargin	Thap	DMSO	100 – 350 nM	150 nM	Cayman Chemical/ 67526–95-8
Histone methyltransferase inhibitor	3-Deazaneplanocin A	DZNep	DMSO	0.025 – 2 μM	2 μM	ApexBio/ 120964–45-6
Histone acetyltransferase inhibitor	Garcinol	Gar	DMSO	5 – 100 μM	5 μM	Cayman Chemical/ 78824–30-3
Histone demethylase inhibitor	GSK-J4	GSK-J4	DMSO	5 – 10 μM	10 μM	Cayman Chemical/ 1373423–53-0

[≠]HC toxin concentration range tested by Li et al. (2015a, b); range finding experiments for these chemicals were not repeated in this study.

The unshaded group consists of HDACi. The lightly shaded group contains non-HDACi toxicants with various MOAs. The darkest group contains non-HDACi compounds that inhibit histone modifying enzymes.

Table 3.

External validation results of the probability analysis, principal component analysis, hierarchical clustering, and the Running Fisher test for the TGx-HDACi transcriptomic biomarker.

External Validation Compound	Mode of Action	Cellular HDAC activity assay*	Probability Analysis	Principal Component Analysis	Hierarchical Clustering	Running Fisher
Entinostat	Class I HDACi	HDACi	HDACi	HDACi	HDACi	HDACi
HC Toxin	Pan-HDACi	HDACi	HDACi	HDACi	HDACi	HDACi
Pracinostat	Pan-HDACi	HDACi	HDACi	HDACi	HDACi	HDACi
Valproic acid	Pan-HDACi	HDACi	HDACi	HDACi	HDACi	HDACi
Docetaxel	Tublin Inhibitor	Non-HDACi	Non-HDACi	Non-HDACi	Non-HDACi	Non-HDACi
Methotrexate	Antifolate	Non-HDACi	Non-HDACi	Non-HDACi	Non-HDACi	Non-HDACi
Arabinofuranosyl cytidine	Nucleotide analogue	Non-HDACi	Non-HDACi	Non-HDACi	Non-HDACi	Non-HDACi
Thapsigargin	ER Ca2+ ATPase inhibitor	Non-HDACi	Non-HDACi	Non-HDACi	Non-HDACi	Non-HDACi
3-Deazaneplanocin A (DZnep)	Histone methyltransferase inhibitor	Non-HDACi	Non-HDACi	Non-HDACi	Non-HDACi	Non-HDACi
Garcinol	Histone acetyltransferase inhibitor	HDACi	Non-HDACi	Non-HDACi	Non-HDACi	Non-HDACi
GSK-J4	Histone demethylase inhibitor	Non-HDACi	Non-HDACi	Non-HDACi	Non-HDACi	Non-HDACi

*HDACi designation indicates statistically significant reduction (One-way ANOVA, Dunnett's post-hoc; p-value >0.05) in HDAC activity compared to HDAC activity in cells treated with vehicle solvent.